Sequential Metal Binding by the RING Finger Domain of BRCA1[†]

Pamela C. Roehm and Jeremy M. Berg*

Department of Biophysics and Biophysical Chemistry, The Johns Hopkins University School of Medicine, 725 North Wolfe Street, Baltimore, Maryland 21205

Received April 14, 1997; Revised Manuscript Received June 13, 1997[⊗]

ABSTRACT: Analysis of the amino acid sequence encoded by the familial breast and ovarian cancer susceptibility gene, BRCA1 [Miki et al. (1994) *Science 266*, 66−71], revealed the presence of an amino-terminal RING finger domain, a zinc binding motif found in a variety of proteins. Previously determined structures of two RING finger peptides from other proteins revealed that each RING finger sequence forms a single domain that includes two interleaved metal binding sites. One is a four-cysteine site comprised of metal binding residues 1, 2, 5, and 6 (in terms of position along the amino acid sequence) (site 1) and the other is a three-cysteine, one-histidine site involving metal binding residues 3, 4, 7, and 8 (site 2). We have characterized the metal binding and metal-dependent folding properties of peptides encompassing the BRCA1 RING finger. Using cobalt(II) as a spectroscopic probe, we have found that metal binding is sequential, with site 1 becoming nearly fully occupied prior to metal binding to site 2. More detailed thermodynamic analysis as well as studies of a variant peptide revealed that metal binding appears to be *anticooperative* with dissociation constants of 3×10^{-8} M for site 1, 5×10^{-7} M for site 2 with site 1 unoccupied, and 8×10^{-6} M for site 2 when site 1 is occupied. Circular dichroism spectroscopic studies revealed that the BRCA1 RING finger peptide is somewhat structured at pH 7 in the absence of metal ions, with further structural changes occurring after the metal binding.

The familial breast and ovarian cancer susceptibility gene BRCA1 encodes a protein of 1863 amino acids (Miki et al., 1994). Only one region of the BRCA1 sequence was found to possess significant similarity to other known gene products; namely, a 56 amino acid sequence at the amino terminus that encodes a RING finger domain (Miki et al., 1994). Several lines of evidence indicate that the RING finger domain of BRCA1 is important for function. First, all of the differentially spliced mRNAs encoded by the BRCA1 gene contain the exons that encode the RING finger (Miki et al., 1994; Xu et al., 1995). Second, missense mutations that would modify cysteine ligands from the RING finger domain have been linked to the increased incidence of breast and ovarian cancer in multiple unrelated families (Shattuck-Eidens et al., 1995). Third, although the murine BRCA1 homolog is only 60% identical to the human protein overall, the proteins are 100% identical in the RING finger region (Abel et al., 1995; Sharan et al., 1995). Fourth, another RING finger domain-containing protein has been identified that interacts specifically with fragments of the BRCA1 protein that include the RING finger (Wu et al., 1996).

Unfortunately, knowledge that the BRCA1 gene encodes a RING finger gives little insight into the function of the protein. RING finger domains have been found in many proteins of greatly disparate function, including proteins involved in the regulation of gene expression, DNA repair and recombination, and peroxisome assembly [reviewed in Schwabe and Klug (1993), Borden and Freemont (1996), and Saurin et al. (1996)]. However, the functional role(s) of the RING finger regions in these proteins is unknown in most cases. One exception is the RING finger domain of RAG1, which, in combination with adjacent regions, has been shown to form a specific dimerization domain (Rodgers et al., 1996).

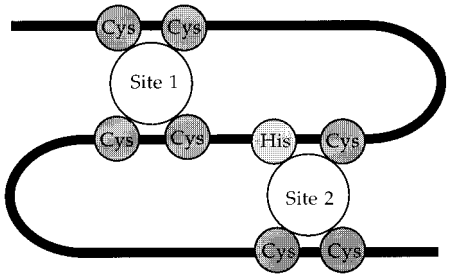

FIGURE 1: Schematic structure of a RING finger domain showing the two interleaved metal binding sites.

The metal binding properties of some RING finger domains have been investigated in a preliminary manner. It is well-established that RING fingers bind cobalt(II), zinc-(II), and cadmium(II) (Lovering et al., 1993; von Armin & Deng, 1993; Upton et al., 1994). The RING (or, alternatively, C_3HC_4) domain includes two apparently tetrahedral metal binding sites formed by alternating pairs of the amino acid ligands, with the first and third pairs of cysteines forming one site and the second and fourth pairs of metal binding residues forming the other (Barlow et al., 1994) as shown in Figure 1. The solution structures of RING finger domains from the equine herpesvirus type 1 immediate-early gene product EHV-63 and that of the acute promyelocytic leukemia protooncoprotein PML have been reported and show similar folding topologies (Barlow et al., 1994; Borden et al., 1995). However, while the core of the domain is maintained, there are significant differences between the two structures that may be functionally important.

In order to provide a basis for understanding the structural and functional properties of the BRCA1 RING finger

[†] This work was supported by a Breast Cancer Program planning grant from the National Cancer Institute.

[⊗] Abstract published in *Advance ACS Abstracts,* August 1, 1997.

S0006-2960(97)00863-5 CCC: $14.00 © 1997 American Chemical Society

Table 1: Sequence of the BRCA1 RING Finger Aligned with Those from Selected Other RING Finger Domains[a]

	3 26
BRCA1 (22-77)	LE**C**PI**C**LELIKE-PVSTK**C**D**H**IF**C**KF**C**MLLKLNQKKGPSQ**C**PL**C**KNDITKRSLQEST
IEEHV (6-63)	ER**C**PI**C**LEDPSNYPMALP**C**L**H**AF**C**YV**C**ITRWI---RQNPT**C**PL**C**KVPVESVVHTIES
PML (55-104)	LR**C**QQ**C**QAEAKC-PKLLP**C**L**H**TL**C**SG**C**LEASG------MQ**C**PI**C**QAPWPLGADTPAL
RING1 (17-72)	LM**C**PI**C**LDMLKNTMTTKE**C**L**H**RF**C**SD**C**IVTAL--RSGNKE**C**PT**C**RKKLVSKRSLRPD
RAG1 (291-334)	IS**C**QI**C**EHILAD-PVETN**C**K**H**VF**C**RV**C**ILRCL--KVMGSY**C**PS**C**RYPCFPTDLESPV

[a] Presumed metal binding residues are shown in boldface type. The positions of the two cysteine residues changed to alanine in BRCA1-Δsite1 are indicated.

domain, we have examined the metal binding and metal-dependent folding properties of a peptide corresponding to the BRCA1 RING finger region. The BRCA1 RING finger peptide was titrated with cobalt(II) and the binding processes were followed by absorption spectroscopy. The spectroscopic properties of cobalt(II) make it a useful probe for zinc sites in proteins; cobalt(II) forms complexes with zinc-binding peptides that are isostructural with the corresponding zinc(II) complexes although binding affinities are generally 3−4 orders of magnitude lower for cobalt than for zinc (Krizek et al., 1993). Changes in the shape of the absorption features in the course of the titration revealed that the two metal binding sites bind cobalt(II) with different affinities and that metal binding is not an all-or-none process for the domain. In order to extract more information about the metal binding processes, we applied factor analysis (Malinowski, 1991) to the absorption spectral data obtained from this titration. A model in which metal binding is sequential and anticooperative appears to describe the metal binding results most consistently. Sequential (rather than concerted) saturation of the two metal sites is surprising in light of the three-dimensional structures of RING finger domains, which reveal that the two sites are part of a single folded unit.

MATERIALS AND METHODS

Materials. A peptide comprised of amino acids 22−77 of the BRCA1 protein was synthesized by solid-phase chemical methods. This sequence was chosen on the basis of alignment with the sequence of the EHV-63 RING finger peptide used to obtain the solution structure (Barlow et al., 1994). The alignment of selected RING finger domains are shown in Table 1. The peptide was synthesized using Fmoc[1] chemistry on a Milligen/Biosearch 9050 peptide synthesizer, reduced with excess dithiothreitol, and purified by reversed-phase HPLC. The purity and identity of the peptide were examined by SDS-polyacrylamide gel electrophoresis and mass spectrometry (MALDI), revealing >95% apparent purity. Peptide samples were stored in an atmosphere of 5−8% hydrogen in nitrogen to avoid cysteine oxidation. The concentration of the peptide used in each measurement was estimated through absorption spectroscopic measurements of the peptide saturated with cobalt(II). An extinction coefficient of 1100 M^{-1} cm^{-1} at 695 nm was determined by quantitative amino acid analysis and was consistent with values determined by computer analysis of metal titration experiments. A variant peptide with cysteine residues at positions 3 and 26 simultaneously changed to alanine (referred to as BRCA1-Δsite1) was synthesized, purified, and characterized by the same methods.

Optically Monitored Cobalt(II) Titrations. Cobalt titrations were performed on BRCA1 peptides monitored by optical spectroscopy over a range of 200−890 nm on a Perkin-Elmer Lambda 9 spectrophotometer at 25 °C. Spectra in the region from 600 to 890 nm were utilized for the spectral analysis as this region is free of absorption from unbound cobalt(II). Peptide concentrations were between 25 and 32 μM in 100 mM HEPES buffer, pH 7.0. During these titrations, the cobalt concentration was raised from 0 to 15 times that of the peptide in a stepwise manner.

Circular Dichroism Spectroscopic Studies. Circular dichroism spectroscopy was performed on an Aviv spectrophotometer in either 5 mM Tris-HCl or 5 mM sodium phosphate buffer, pH 7.0, at peptide concentrations between 7 and 10 μM. Spectra were measured with metal ion concentrations ranging from 0 to 50 μM.

Analysis of Spectra. We first analyzed the data from the cobalt titrations using factor analysis (Malinowski, 1991). In this method, a data matrix (D_{obs}) is generated in which the row indices run over titration points at different cobalt(II) concentrations and the column indices correspond to wavelength values. The elements of this matrix are the absorbance values at each wavelength. Multiplication of this matrix by its transpose generates the covariance matrix, C

$$C = D_{obs}D^{T}_{obs} \quad (1)$$

which retains the complete description of the titration in a more compact form. Diagonalization of the covariance matrix produces a matrix of eigenvectors (V) and their associated eigenvalues. The eigenvalues give the relative importance of the eigenvector in the reconstruction of the original data matrix. The eigenvectors can be used to calculate basis spectra (R) by multiplying the transpose of the eigenvector matrix by the data matrix:

$$R = V^{T}D_{obs} \quad (2)$$

These basis vectors can be used to evaluate the number of eigenvectors needed to describe the data within the limits of experimental error by calculating the linear least-squares difference (Q) between the reconstructed data matrix (D_{calc}) and the observed data matrix (D_{obs}) at each cobalt(II) concentration and wavelength:

[1] Abbreviations: Fmoc, *N*-fluorenylmethoxycarbonyl; HPLC, high-performance liquid chromatography; MALDI, matrix-assisted laser desorption ionization; HEPES, 4-(2-hydroxyethyl)-1-piperazineethanesulfonic acid.

$$Q = \sum (D_{obs} - D_{calc})^2 \quad (3)$$

where the sum runs over all wavelengths and cobalt(II) concentrations.

For all data sets, two basis vectors were needed to describe the optical titration data adequately, indicating that two absorbing species with different dependences on peptide and metal concentration were present. The coefficients representing the contributions of the two basis spectra to the data set at cobalt(II) concentration i are given by $f_1o(i)$ and $f_2o(i)$.

The above process serves to compress the data and to evaluate the number of spectroscopically distinct components but does not provide insight into the absorption spectra or other properties of the chemical components. In order to obtain such information, models for the chemical behavior of the absorbing species must be included. Two models for metal binding by the RING finger domain were investigated. In the first model, the sites are independent so that $K_1 = K_4$ and $K_2 = K_3$ in Figure 3. In the second model, the possibility of cooperativity between the two sites was considered so that the affinity of one site for metal ion could depend on the occupancy of the other site; that is, $K_2 \neq K_3$.

These models were fitted to the observed data. For both models, it was assumed that the absorption spectrum due to the complex at one site was independent of the occupancy of the other site. Estimates for the equilibrium constants were used to evaluate the concentrations of the individual species at each set of experimental conditions [peptide concentration, cobalt(II) concentration]. The absorption spectra for the cobalt(II) complexes of the two sites were estimated as linear combinations of the basis vectors obtained from the eigenvalue analysis above. From these estimates, the contribution of each basis spectrum to the observed data could be calculated from

$$f_1c(i) = c_{11}\{[PM_1](i) + [PM_1M_2](i)\} + c_{12}\{[PM_2](i) + [PM_1M_2](i)\} \quad (4)$$

$$f_2c(i) = c_{21}\{[PM_1](i) + [PM_1M_2](i)\} + c_{22}\{[PM_2](i) + [PM_1M_2](i)\} \quad (5)$$

where $[PM_1]$ is the concentration of the species with metal bound only in site 1, $[PM_2]$ is the concentration of the species with metal bound only in site 2, and $[PM_1M_2]$ is the concentration of the species with metal bound both in sites 1 and 2, and the index i runs over the data points at different cobalt(II) concentrations under consideration.

These values can then be compared with the observed contributions of each basis spectrum. The quantity

$$F = \sum_i \{[f_1o(i) - f_1c(i)]^2 + [f_2o(i) - f_2c(i)]^2\} \quad (6)$$

was then minimized with respect to the coefficients c_{ij} ($i, j = 1, 2$), the equilibrium constants associated with each model, and a factor accounting for the precise concentration of active peptide. Minimization was accomplished through the use of the simplex method (Nelder & Mead, 1965). After completion of this minimization procedure, absorption spectra for the pure components [cobalt(II) bound in site 1, cobalt(II) bound in site 2] and values for the equilibrium constants were obtained. Standard deviations for the equilibrium constants were estimated from the sensitivity of the agreement factor F to changes in the individual parameters.

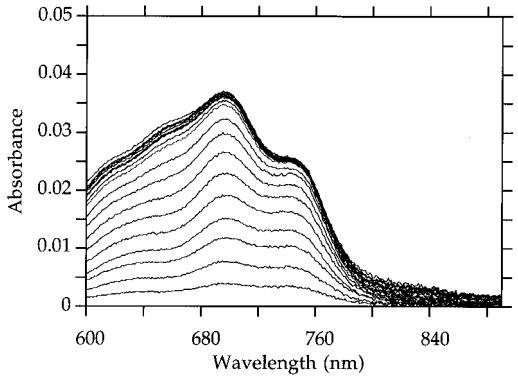

FIGURE 2: Optically monitored titration of the BRCA1 RING finger peptide with cobalt(II). Note that the shape of the absorption envelope changes during the titration.

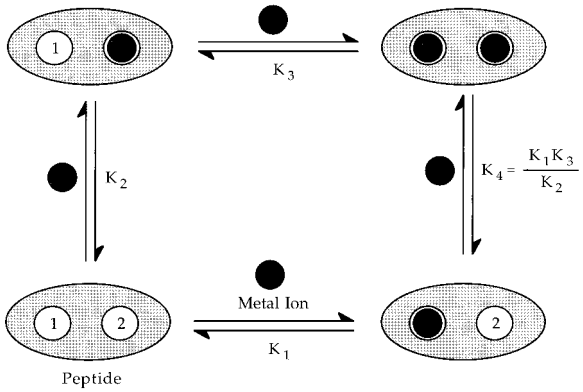

FIGURE 3: Thermodynamic scheme for cooperative metal binding to the two sites within the RING finger domain.

Analysis of the CD-monitored titration spectra was performed in a similar manner, with the inclusion of fixed weighting coefficients for the contribution of the apopeptide to the overall CD spectra. The CD data were included along with those from the UV−visible titration to obtain a single set of equilibrium constants that best fit all of the observed data.

RESULTS

Titration of the BRCA1 RING finger peptide with cobalt(II) resulted in the absorption spectra shown in Figure 2. These spectra were analyzed by factor analysis. As indicated by the changes in the shape of the absorption envelope during the titration, two component spectra were necessary to account for the observed spectra. The model in which the two sites were assumed to be thermodynamically independent of one another was fit to the data. A suitable fit was obtained using this model when one site had an affinity approximately 50-fold higher than that for the other site. The absorption spectra of the individual components deduced from this analysis are shown in Figure 4. The intensities of these spectra are consistent only with the expected four-coordinate, approximately tetrahedral, geometries. The shapes and positions of the absorption envelopes clearly indicate that the higher affinity site has four cysteinate ligands, based on comparison with other cobalt(II) complexes with various combinations of cysteine and histidine ligands (Krizek et al., 1993). The spectrum of the lower affinity site is consistent with coordination by three cysteinate and one histidine residues.

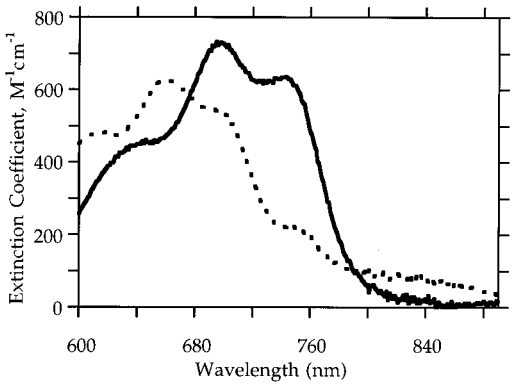

FIGURE 4: Absorption spectra for the two cobalt(II) complexes within the BRCA1 RING finger peptide deduced from factor analysis. Higher affinity site, solid line; lower affinity site, dotted line. On the basis of the positions of the absorption features, the higher affinity site corresponds to site 1 and the lower affinity site to site 2 in Figure 1.

A second model that includes the possibility of cooperativity in binding between the two metal binding sites yielded a fit with a similar level of agreement. This model includes one additional variable parameter but no significant improvement in the fit was obtained compared with that from the first model. In addition, the observed and calculated contributions due to the two spectral components were very similar and essentially identical spectra for cobalt(II) bound to the two sites were obtained. Thus, these initial data did not allow discrimination between the two models.

To further evaluate these models, a peptide was synthesized in which Cys 3 and Cys 26, two of the metal ligands in the higher affinity site (site 1), were changed to alanine (Figure 1). Titration of this peptide (BRCA1-Δsite1) with cobalt(II) resulted in the spectra shown in Figure 5a. The shape of this spectrum did not change during the titration and more detailed analysis revealed that only a single component was necessary to describe these data. The observed spectrum for BRCA1-Δsite 1 and the component spectrum for the lower affinity site are compared in Figure 5b,c. The similarity in spectral position and shape provides independent confirmation of the assignment of sites 1 and 2 and validates the factor analysis approach. The increase in the intensity of this absorption spectrum as a function of added cobalt(II) concentration was fitted to yield a dissociation constant of 4.5 ($\pm$ 0.3) $\times$ 10^{-7} M. With the assumption that this value reflected the intrinsic affinity of site 2 when site 1 is unoccupied (corresponding to K_2 in Figure 3), the cooperative model was again fitted to observed data for the wild-type peptide. A fit with a similar level of agreement to those above was obtained. The experimentally deduced and calculated values for the concentrations of the complexes of cobalt(II) bound in the two sites are shown in Figure 6a. A plot of the deduced concentrations of the species with cobalt(II) bound in one or both sites is shown in Figure 6b. The dissociation constants deduced from this fit are shown in Table 2.

A titration of the BRCA1 RING finger peptide with cobalt(II) monitored by circular dichroism spectroscopy is shown in Figure 7a. Even in the absence of metal ion, the CD spectrum reveals evidence for some structure, based on the negative circular dichroism near 220 nm. The factor analysis was expanded to include these data in addition to those from the UV−visible titration. Two components were found to be necessary to describe the CD spectra throughout the titration. The CD spectrum of the apopeptide was included with fixed coefficients. A total of four variable coefficients were included to describe the CD spectra of the peptide with cobalt(II) bound in site 1 and the peptide with cobalt(II) bound in both sites. The concentration of the complex with

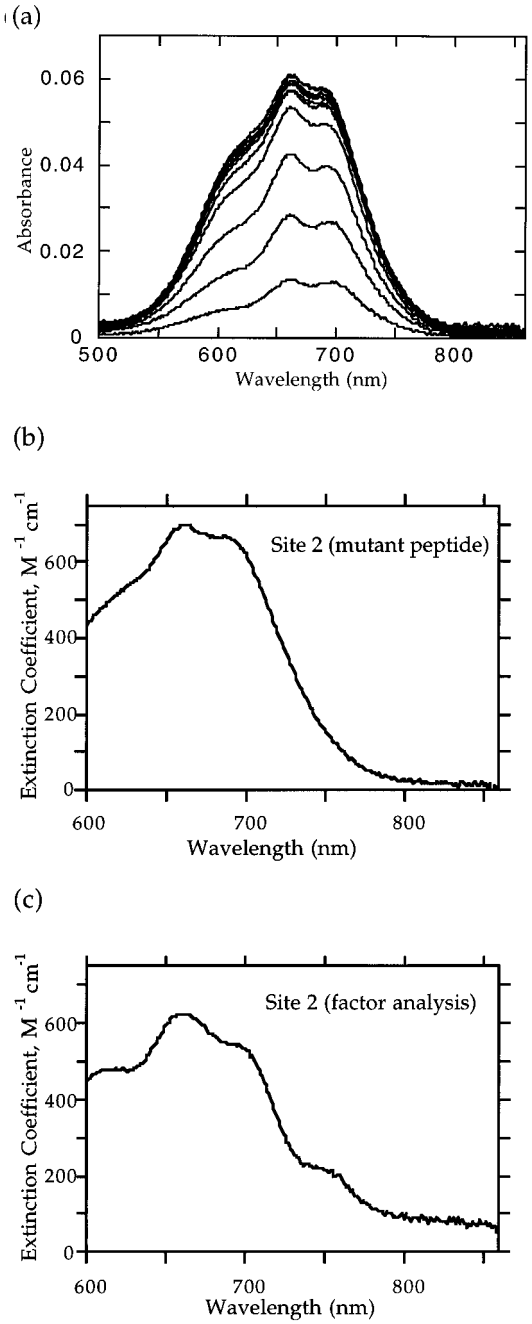

FIGURE 5: (a) Results of a cobalt(II) titration of the BRCA1-Δsite1 peptide, which has the metal binding capability of site 1 neutralized by mutation of two cysteines to alanine. (b) Absorption spectrum for cobalt(II) bound in site 2 from BRCA1-Δsite1. (c) Absorption spectrum for cobalt(II) bound in site 2 deduced from factor analysis.

Table 2: Metal Binding Constants Deduced from Factor Analysis and Fitting[a]

K_1	2.6×10^{-8} M	log (K_1)	-7.6 ± 0.7
K_2	4.5×10^{-7} M	log (K_2)	-6.4 ± 0.3
K_3	7.9×10^{-6} M	log (K_3)	-5.1 ± 0.1

[a] The equilibrium constants are defined in Figure 3 and are shown as dissociation constants. Log values and their estimated standard deviations are also given.

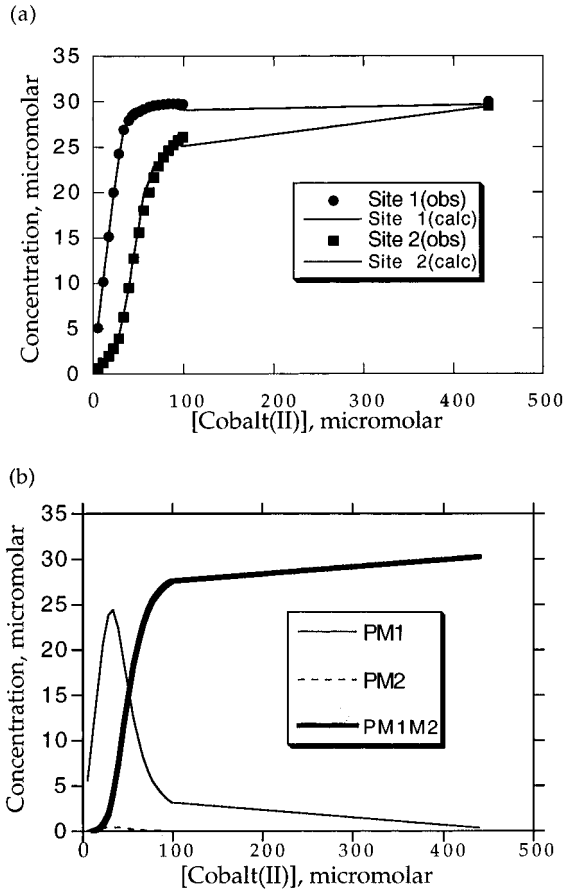

FIGURE 6: (a) Comparison of the contributions of absorption due to site 1 and site 2 deduced from the experimental spectra with those derived from the anticooperative binding model. (b) Concentrations of the singly and doubly metalated peptide complexes as a function of total cobalt(II) concentration calculated from the anticooperative binding model. Peptide with cobalt in site 1 only, dotted line; peptide with cobalt in site 2 only, dashed line; peptide with cobalt in both site 1 and site 2, solid line.

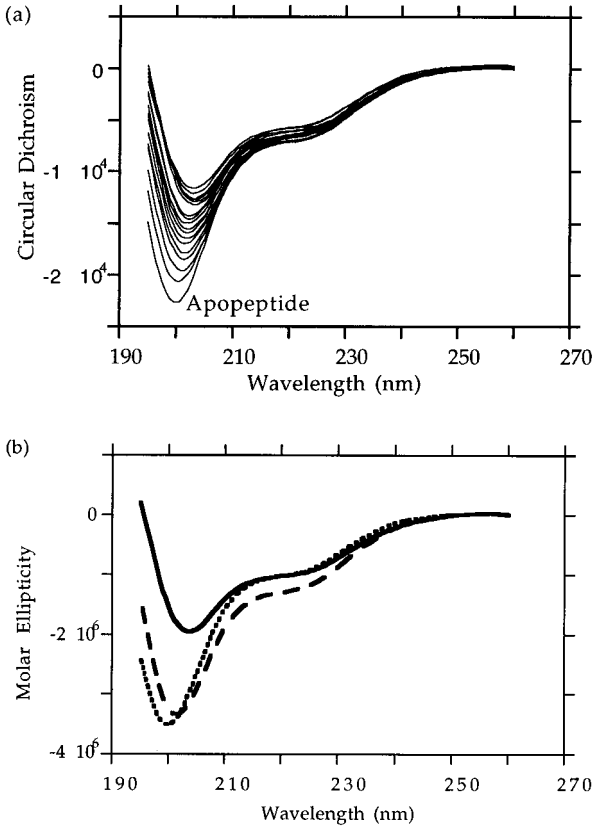

FIGURE 7: (a) Results of a cobalt(II) titration of the BRCA1 RING finger peptide monitored by CD spectroscopy. Values are given as molar ellipticities per mole of amino acids. (b) CD spectra of the BRCA1 RING finger peptide and its cobalt(II) complexes deduced by factor analysis. Values are given as molar ellipticities per mole of peptide. Apopeptide, dashed line; peptide with cobalt in site 1 only, dotted line; peptide with cobalt in both site 1 and site 2, solid line.

cobalt(II) only in site 2 was sufficiently low that this species did not contribute significantly to the CD spectra. The simplex minimization was repeated, and no significant changes in the equilibrium constants occurred. The deduced CD spectra of the various species are shown in Figure 7b.

DISCUSSION

The three-dimensional structures of the RING finger domains reported to date show a domain with two interleaved metal binding sites. The interwoven nature of this structure suggests that metal binding would occur in an all-or-none fashion, that is, once a metal ion binds to one site, a metal ion would bind to the other site within the same polypeptide with high probability. We investigated the metal binding properties of a peptide corresponding to the RING finger domain from the tumor suppressor gene product BRCA1 to test for this positive cooperativity in metal binding. In contrast to the above expectations, we found that metal binding is thermodynamically *sequential* with cobalt(II) almost saturating one of the two sites in each polypeptide prior to binding to the other site. Analysis of the absorption spectra due to cobalt(II) bound to the two sites revealed that the higher affinity site is comprised of four cysteinate ligands whereas the lower affinity site has three cysteinate and one histidine ligands.

On the basis of studies of the wild-type peptide alone, the sequential binding could have been due either to a large difference in the intrinsic affinities of the two sites or to site−site cooperative interactions that favored sequential binding. To distinguish between these two possibilities, we examined the metal binding properties of BRCA1-Δsite1 in which the metal binding capacity of the higher affinity site was destroyed. Analysis of a cobalt(II) titration of this peptide revealed that BRCA1-Δsite1 has an intermediate level of affinity, lower than that for the high-affinity site but higher than that deduced for site 2 when site 1 is occupied. Thus, metal binding is anticooperative, with the affinity of site 2 decreasing by approximately 20-fold when a metal ion binds to site 1.

The effects of metal binding on peptide folding was probed through the use of CD spectroscopy. The results of a cobalt(II) titration of the BRCA1 RING finger peptide monitored by CD could be simultaneously fit with results from titrations monitored by visible absorption to yield deduced CD spectra for species with cobalt(II) bound to site 1 and with cobalt(II) bound in both sites. More substantial changes in the CD spectra occurred upon binding the second cobalt(II) ion.

These observations can be summarized as follows. The apopeptide includes some elements of structure. Upon binding a metal ion to site 1, the peptide becomes somewhat more structured and, perhaps, more rigid in a manner that affects the regions involved in forming site 2. This, in turn,

increases the difficulty in binding a metal ion to site 2, leading to the observed anticooperativity.

The biological significance of this sequential metal binding remains to be determined. The importance of the mechanism of metal binding and the potential role(s) of domains not completely saturated with metal ions has not been established for any class of zinc binding domain. However, two pieces of evidence suggest that this sequential binding is a general characteristic of RING finger domains. First, a published titration of the PML RING finger peptide (Borden et al., 1995) shows shape changes similar to those we observed for the BRCA1 peptide. Second, metal binding studies of fragments including the RING finger from *Arabidopsis* COP1 revealed that one of two bound zinc ions was quite resistant to removal by chelators whereas the other was more labile (von Armin & Deng, 1993). As researchers attempt to unravel the biological roles of BRCA1 and other RING finger-containing proteins, knowledge of these metal binding properties may prove important. Perhaps RING finger domains with only one metal binding site filled have different functional roles than those fully saturated with metal ions. In this light, it is interesting to note that RING finger-like domains have been identified that appear to be lacking the residues that correspond to site 2 (Kalish et al., 1996).

ACKNOWLEDGMENT

We are grateful to Doug Barrick, Wes McDermott, and Nicholas Goffeney for useful discussions.

REFERENCES

Abel, K., Xu, J., Yin, G., Lyons, R., Meisler, M., & Weber, B. (1995) *Hum. Mol. Genet. 4*, 2265−2273.

Barlow, P., Luisi. B., Milner, A., Elliot, M., & Everett, R. (1994) *J. Mol. Biol. 237*, 201−211.

Borden, K., & Freemont, P. (1996) *Curr. Opin. Struct. Biol. 6*, 395−401.

Borden, K., Boddy, M., Lally, J., O'Reilly, N., Matrin, S., Howe, K., Solomon, E., & Freemont, P. (1995) *EMBO J. 14*, 1532−1541.

Kalish, J. E., Keller, G. A., Morrell, J. C., Mihalik, S. J., Smith, B., Cregg, J. M., & Gould, S. J. (1996) *EMBO J. 15*, 3275−3285.

Krizek, B. A., Merkle, D. L., & Berg, J. M. (1993) *Inorg. Chem. 32*, 937−940.

Lovering, R., Hanson, I., Borden, K, Martin, S. O'Reilly, N., Evan, G., Rahman, D., Pappin, D., Trowdale, J., & Freemont, P. (1993) *Proc. Natl. Acad. Sci. U.S.A. 90*, 2112−2116.

Malinowski, E. (1991) *Factor Analysis in Chemistry*, 2nd ed., John Wiley & Sons, Inc., New York.

Miki, Y., Swensen, J., Shattuck-Eidens, D., Futreal, P. A., Harshman, K., Tavtigian, S., Liu, Q., Cochran, C., Bennett, L. M., Ding, W., Bell, R., Rosenthal, J., Hussey, C., Tran, T., McClure, M., Frye, C., Hattier, T., Phelps, R., Haugen-Strano, A., Katcher, H., Yakumo, K., Gholami, Z., Shaffer, D., Stone, S., Bayer, S., Wray, C., Bogden, R., Dayananth, P., Ward, J., Tonin, P., Narod, S., Bristow, P. K., Norris, F. K., Helvering, L., Morrison, P., Rosteck, P., Lai, M., Barrett, J. C., Lewis, C., Neuhausen, S., Cannon-Albright, L., Goldgar, D., Wiseman, R., Kamb, A., & Skolnick, M. H. (1994) *Science 266*, 66−71.

Nelder, J. A., & Mead, R. (1965) *Comput. J. 7*, 308−313.

Rodgers, K., Bu, Z., Fleming, K., Schatz, D., Engelman, D., & Coleman, J. (1996) *J. Mol. Biol. 260*, 70−84.

Saurin, A., Borden, K. Boddy, M, & Freemont, P. (1996) *Trends Biochem. Sci. 21*, 208−214.

Schwabe, J., & Klug, A. (1994) *Nat. Struct. Biol.* 1, 345−349.

Sharan, S., Wims, M., & Bradley, A. (1995) *Hum. Mol. Genet. 4*, 2275−2278.

Shattuck-Eidens, D., McClure, M., Simard, J., Labrie, F., Narod, S., Couch, F., Hoskins, K., Weber, B., Castilla, L., Erdos, M., Brody, L., Friedman, L., Ostermeyer, E., Szabo, C., King, M., Jhanwar, S., Offit, K., Norton, L., Gilewski, T., Lubin, M., Osborne, M., Black, D., Boyd, M., Steel, M., Ingles, S., Haile, R., Lindblom, A., Olsson, H., Borg, A., Bishop, D. T., Solomon, E., Radice, P., Spatti, G., Gayther, S., Ponder, B., Warren, W., Stratton, M., Liu, Q., Fujimura, F., Lewis, C., Skolnick, M. H., & Goldgar, D. E. (1995) *J. Am. Med. Assoc. 273*, 535−541.

Upton, C., Schiff, L., Rice, A., Dowdeswell, T., Yang, X., & McFadden, G. (1994) *J. Virol. 68*, 4186−4195.

von Arnim, A., & Deng, X. (1993) *J. Biol. Chem. 268*, 19626−19631.

Wu, L. C., Wang, Z. W., Tsan, J. T., Spillman, M. A., Phung, A., Xu, X. L., Yang, M. W., Hwang, L., Bowcock, A. M., & Baer, R. (1996) *Nature Genet. 14*, 430−440.

Xu, C., Brown, M., Chamber, J., Griffiths, B. Nicolai, H., & Solomon, E. (1995) *Hum. Mol. Genet. 4*, 2259−2264.

BI970863D